Available online at www.sciencedirect.com
ScienceDirect
Journal of Energy Chemistry 22(2013)341–346
JEC JOURNAL OF ENERGY CHEMISTRY
www.elsevier.com/locate/jngc

Hierarchical nanostructured composite cathode with carbon nanotubes as conductive scaffold for lithium-sulfur batteries

Xiaofei Liu, Qiang Zhang*, Jiaqi Huang, Shumao Zhang, Hongjie Peng, Fei Wei*

Beijing Key Laboratory of Green Chemical Reaction Engineering and Technology, Department of Chemical Engineering, Tsinghua University, Beijing 100084, China

[Manuscript received November 20, 2012; revised January 7, 2013]

Abstract

Carbon nanotubes (CNTs) are excellent scaffolds for advanced electrode materials, resulting from their intrinsic sp^2 carbon hybridization, interconnected electron pathway, large aspect ratio, hierarchical porous structures, and low cost at a large-scale production. How to make full utilization of the mass produced CNTs as building blocks for nanocomposite electrodes is not well understood yet. Herein, a composite cathode containing commercial agglomerated multi-walled CNTs and S for Li-S battery was fabricated by a facile melt-diffusion strategy. The hierarchical CNT@S coaxial nanocables exhibited a discharging capacity of 1020 and 740 mAh $\cdot g^{-1}$ at 0.5 and 2.0 C, respectively. A rapid capacity decay of 0.7% per cycle at the initial 10 cycles and a slow decay rate of 0.14% per cycle for the later 140 cycles were detected. Such hierarchical agglomerated CNT@S cathodes show advantages in easy fabrication, environmentally benign, low cost, excellent scalability, and good Li ion storage performance, which are extraordinary composites for high performance Li-S battery.

Key words

carbon nanotubes; lithium sulfur battery; hierarchical nanocomposite; cathode; energy storage

1. Introduction

Chemical energy storage using rechargeable lithium-ion batteries is one of the most important power sources to meet the requirement of rapid increasing demand from portable electronic devices, electrical vehicles, hybrid electrical vehicles, and so on [1]. The rapid innovation on the composite electrode provides the driving force for the continuous improvement on the Li storage performance. Owing to the multiple-electron-transfer electrochemistry of light element-sulfur, the Li-S battery possesses a high theoretical capacity and energy density of 1672 mAh$\cdot g^{-1}$ and 2600 Wh$\cdot kg^{-1}$, respectively [2−5]. However, the practical application of sulfur cathode material is hindered by the insulating nature of S and Li_2S_x ($x = 1$ or 2), the low utilization of active phase, and the rapid capacity degradation [2−6]. Novel electrolyte and advanced cathode materials are urgently anticipated to overcome these technical obstacles.

Nanocarbon materials are of hierarchical porous nanostructure, high electronic conductivity, and tunable surface chemistry [7]. The incorporation of nanocarbon into sulfur cathode gives rise to advanced electrodes with improved reversible charge-discharge capacity and cycling performance. The use of highly ordered mesoporous carbon CMK-3 that constrained sulfur within its channels renders a reversible capacities up to 1320 mAh$\cdot g^{-1}$ [8]. Activated carbon [9], porous carbon [8,10], carbon black [11,12], microporous carbon spheres [13], graphene [14−16], CNTs [17−24], carbon nanofibers [25], CNT/graphene hybrid [26], pyrolyzed polyacrylonitrile-sulfur@MWCNTs [27], and polyaniline coating of CNT/sulfur cathode [28] were demonstrated to be excellent fillers to improve the Li ion storage performance of sulfur materials.

With the rapid progresses on industrial mass production and commercialization of CNTs [29,30], the use of CNTs as energy materials for energy conversion and storage, such as fuel cells [31,32], supercapacitors [33], and Li batteries [1], is very attractive. The proof of concept of CNTs as the framework for advanced Li-S batteries is explored. For instance, the sulfur cathode prepared by mixing 50% sulfur, 20% acetylene black, 20% multi-walled CNT (MWCNT) and

* Corresponding authors. Tel: +86-10-6278-9041; Fax: +86-10-6277-2051; E-mail: zhang-qiang@mails.tsinghua.edu.cn (Q. Zhang), wfdce@tsinghua.edu.cn (F. Wei)

This work was supported by National Basic Research Program of China (973 Program, 2011CB932602), Research Fund for the Doctoral Program of Higher Education of China (20120002120047), and China Postdoctoral Science Foundation (2012M520293).

10% polyvinylidene fluoride (PVDF) offers an initial discharge capacity 485 mAh·g^{-1} [34]. A composite cathode containing single-wall CNT@S nanocables offered reversible capacities of 676 mAh·g^{-1} for the 1st discharging at 0.5 C, and 441 mAh·g^{-1} for the 100th discharging at 1.0 C [35]. The sulfur encapsulated by hollow carbon nanofibers provided quite high capacities of ca. 1580 and 730 mAh·g^{-1} at 0.2 C for the 1st and 150th cycles, respectively [25]. Flexible nanostructured sulfur-CNTs [18,36], high sulfur loading (90%) CNT composite [37], hierarchical architectural CNT nano/microsphere [20] as well as carbon fiber nonwoven with CNT branches [38] were illustrated to be effective sulfur/carbon materials with large pores for excellent Li ion storage performance. Recently, it is found that the CNT-based composite cathode can become market ready as 18650 cells with a low cost of CNTs [38].

In this contribution, CNTs mass-produced by fluidized bed chemical vapor deposition with a low cost (less than 100 \$·kg^{-1}) [29] were employed as scaffolds to fabricate hierarchical composite cathode for Li-S battery. Beneficial from the sp^2 carbon nanostructure, large aspect ratio, interconnected electron pathway, and hierarchical porous agglomerates of the CNTs, the composite cathode consisting of CNT@S coaxial nanocables offers excellent reversible Li ion storage performance with excellent cycling stability.

2. Experimental

2.1. Fabrication of CNT@sulfur cathodes

The CNTs were mass produced by nano-agglomerated fluidized bed technology. A facile co-heating was employed to load the electrochemically active sulfur phase into the CNT framework. In a typical procedure, the sulfur powder was mixed with the CNTs by ball milling. The as-obtained mixtures were set in a sealed bottle. The bottle was heated to 155 °C and maintained for 1 h, which allowed sulfur to immerse into the CNT scaffold and form CNT@sulfur composite cathode.

2.2. Structure characterizations

A JSM 7401F scanning electron microscopy (SEM, JEOL Ltd., Tokyo, Japan) at 1.0 kV and a transmission electron microscopy (TEM, JEOL Ltd., Tokyo, Japan) at 120.0 kV were employed to detect the morphology of cathodes. The energy dispersive X-ray spectroscopy (EDX) analysis was performed using an EDAX apparatus. The Raman spectra of the CNT and CNT@S cathodes were recorded using Horiba Jobin Yvon LabRAM HR800 Raman spectrometer (He-Ne laser excitation at 633 nm). The sulfur content of CNT@S electrode was determined by thermogravimetry analysis (TGA) using TGA/DSC1 STAR^e system with N_2 atmosphere and a temperature ramp rate of 10 °C·min^{-1}. The N_2 adsorption-desorption isotherms were collected by a N_2 adsorption analyzer (Autosorb-IQ$_2$-MP-C system) at 77 K. The sample was degassed at a low temperature of 50 °C until a manifold pressure of 2 mm Hg was reached before N_2 adsorption isotherm measurements to avoid the sulfur sublimation. The surface area was determined by the Brunauer-Emmett-Teller (BET) method, and the pore size distribution plot was available by the nonlocal density functional theory and Monte-Carlo method.

2.3. Li storage performance on composite cathode

The CNT@S composite cathode was fabricated with PVDF binder in NMP with a mass ratio of CNT@S : PVDF = 85 : 15. A homogeneously mixed slurry was prepared by magnetic stirred for ca. 24 h. The as-obtained slurry was coated onto a 20 μm thick Al current collector by a doctor blade. The obtained electrode was dried in a vacuum drying oven at 60 °C for 12 h. After that, the foil was punched into 13 mm disks as the working cathodes.

The electrodes were assembled in a two-electrode cells configuration using standard 2025 coin-type cells. 1 mm thick Li metal foil was selected as counter electrodes. Tetraethylene glycol dimethyl ether (TEGDME) with 1 mol·L^{-1} lithium trifluoromethanesulfonate ($LiCF_3SO_2$) and 0.25 mol·L^{-1} lithium nitrate ($LiNO_3$) were used as the electrolyte, and the Celgard 2400^R polypropylene membranes were used as separators. The assembling of cells was conducted in an Ar-filled glove box with oxygen and water contents below 1 ppm. Cyclic voltammogram (CV) measurements were performed on a Solartron 1470E electrochemical workstation at a scan rate of 0.1 mV·s^{-1}. The coin cells were monitored in galvanostatic mode within a voltage range of 1.7−2.8 V using Neware multichannel battery cycler.

3. Results and discussion

The morphologies of CNT@S composite cathode were shown in Figure 1. The cathode presented a three-dimensional multi-stage nanoarchitecture, in which the CNT@S composite heavily entangled with each other, which can be considered a replication of the agglomerated CNTs. The sub-agglomerates of ca. 1 μm were formed due to the strong van der Waals interaction, and these sub-agglomerates tends to further aggregate into large CNT@S agglomerates, some even as large as 400−500 μm [39].

The structure of CNT@S coaxial nanocables can be clearly identified by the TEM images. The sulfur layers with a thickness around 4 nm were uniformly coated on the outer layers of CNTs. In this coaxial structure, CNTs serve as conductive scaffold and the sulfur phase can be used as active components for Li ion storage. The well preservation of agglomerated nanoarchitectures was mainly attributed to the porous raw CNTs, offering interconnected channels for sulfur diffusion at 155 °C. In this case, the sulfur showed the lowest surface tension [8]. Both the conductive network and the porous channel are beneficial for reversible charge-discharge electrochemical reaction in a Li-S battery.

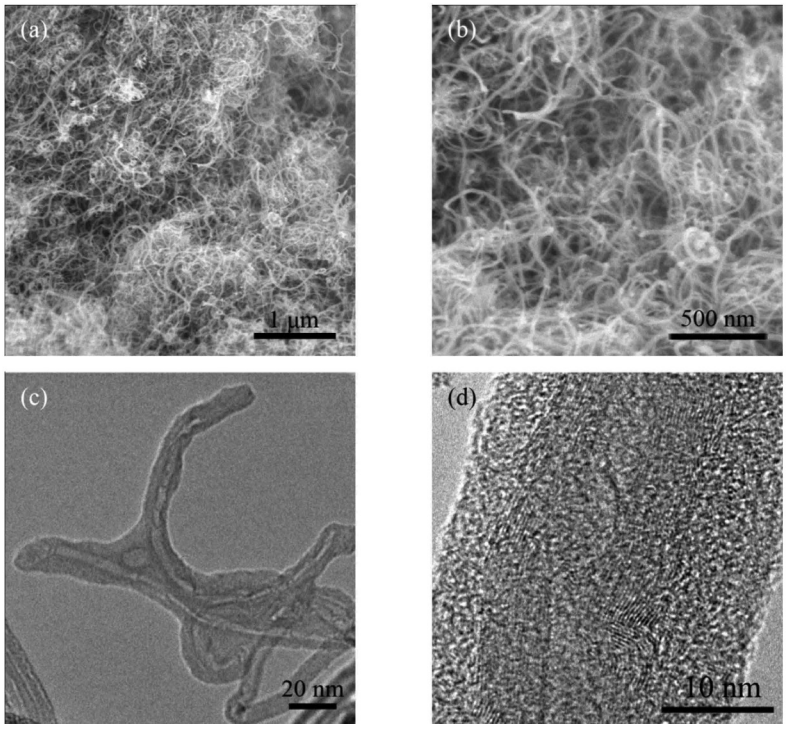

Figure 1. SEM (a, b) and TEM (c, d) images of the CNT@S composite cathode

The amount of sulfur in the composite cathode was determined to be 50 wt% (0.25 mg·cm^{-2} in the electrode) by TGA in N_2 atmosphere. The weight loss peak of sulfur in CNT@S cathode shifted to higher temperature range of 260−350 °C (Figure 2a) than that of the sulfur element. This indicates the sulfur prefers to attach on the outer wall of CNTs in confined space. However, the sulfur peak in the composite is hardly to be detected by Raman spectra (Figure 2b). The XRD patterns of the composite show that the sulfur peak is broadened than that of the crystalline sulfur (Figure 2c). Both of them confirmed the uniform distribution of ultrafine sulfur in the cathode. The sulfur preferred to attach on the hydrophobic sp^2 carbon surface. The N_2 adsorption isotherm indicated that the CNT pores were almost occupied by sulfur (Figure 2d). The decrease in the pore volume from 0.65 to 0.25 cm^3·g^{-1} as well as the specific surface area from 208 to 91 m^2·g^{-1} reconfirmed the occupation of sulfur within the CNTs.

In order to comprehensively investigate the Li ion storage performance of the CNT@S cathode, CV and galvanostatic charge-discharge measurements were carried out. In the CV profile, two main reduction peaks at around 2.44 and 1.95 V were detected during the first cathodic scan (Figure 3), which were assigned to the transformation from sulfur to lithium polysulfides (nS+2Li$^+$+2e$^-$⟶Li$_2$S$_n$, (4⩽n⩽8)) and the reduction of high order lithium polysulfides into lithium sulfides (Li$_2$S$_n$+2(n-1)Li$^+$+2(n-1)e$^-$⟶nLi$_2$S (n<4)), respectively [18]. There are two oxidation peaks at ca. 2.38 and 2.52 V in the subsequent anodic scan, which are correlated with the conversion from lithium sulfide to lithium polysulfide and the oxidation of the polysulfide into element sulfur, respectively. With the addition of $LiNO_3$ in the tetraethylene glycol dimethyl ether (TEGDME) electrolyte, the polarization is more obvious than these in 1, 3-dioxolane : 1, 2-dimethoxyethane (v/v = 1/1) with 1 mol·L^{-1} lithium bis-(trifluoromethanesulfonyl) imide (LiTFSI) electrolyte, which showed two reduction peaks at 2.31 and 2.06 V and two oxidation peaks at 2.24 and 2.36 V, respectively [35]. However, the coulombic efficiency was almost near 100% in the TEGDME with $LiCF_3SO_2$ and $LiNO_3$ electrolyte. The $LiNO_3$ additives were reduced on Li to form insoluble Li_xNO_y species and oxidized the sulfides to Li_xSO_y species that passivate the Li electrodes and prevent the continuous electron transfer from Li to polysulfides in solutions [40]. The enhancement of Li passivation remarkably diminishes the possible reduction in polysulfide species in solutions by the reactive lithium electrodes [40]. Polysulfides in the electrolyte were prevented from contacting with lithium foil directly by the protective film of both inorganic species such as LiN_xO_y and organic species such as ROLi and $ROCO_2Li$ [12,41]. However, deep discharge should be avoided as irreversible reduction of $LiNO_3$ on cathode and a significant slowdown in the electrode reaction kinetics as well as a permanent loss in the reversibility of the Li/S cell occur at around 1.6 V [42]. Therefore, a cut-off voltage of 1.7 V was employed in the electrochemical test.

The reduction and oxidation peaks shown on the CV profile (Figure 3) were well maintained with the increase of cycle number. No obvious change in the intensity and position of the cathodic and anodic scans was observed, except that the first oxidation of the lithium sulfide and the polysulfide shifted to low voltage. This indicated the good electrochemical reversibility for CNT@S cathode during charge/discharge cycles in TEGDME with 1 mol·L^{-1} $LiCF_3SO_2$ and 0.25 mol·L^{-1} $LiNO_3$ as the electrolyte.

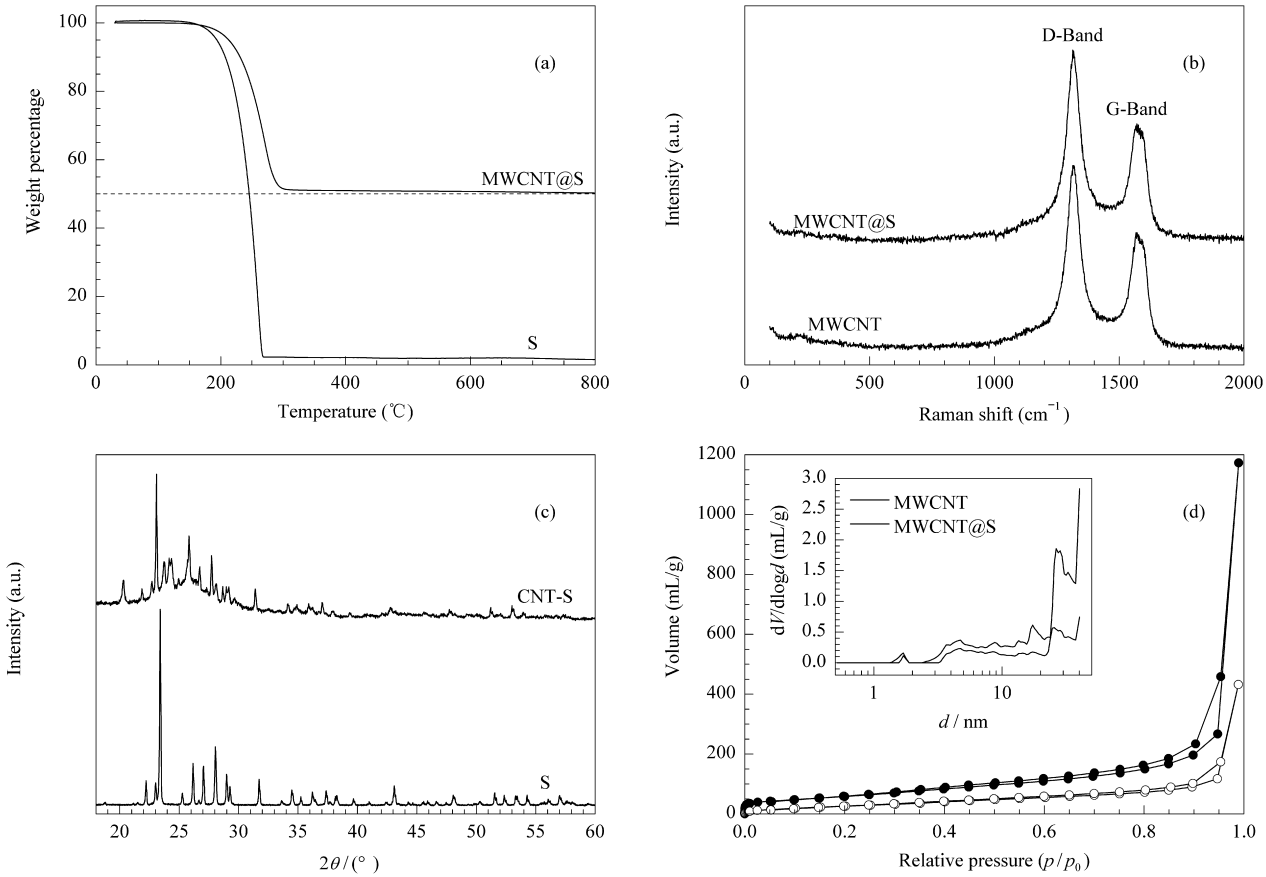

Figure 2. TGA profile (a), Raman spectra (b), XRD patterns (c), and N_2 adsorption isotherms (d) and pore size distributions (inset) of hierarchical CNT@S composite cathode

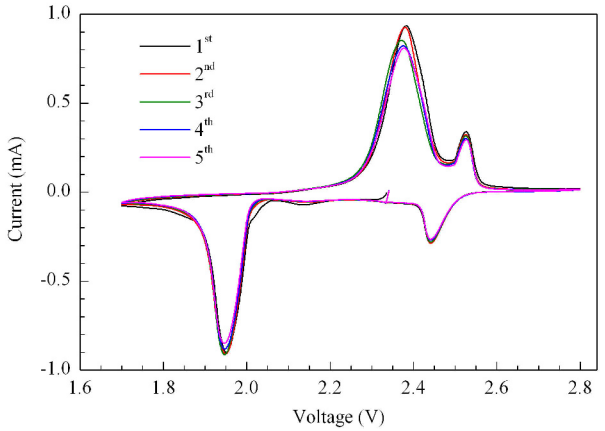

Figure 3. CV profiles of CNT@S composite cathode with a scanning rate of 0.1 mV·s^{-1} in the voltage range from 1.7 to 2.8 V vs. Li/Li$^+$

The cycling performance of CNT@S cathode was shown as Figure 4(a). The 1st and 150th discharging capacities at 1.0 C (0.418 mA·cm^{-2}) were 975 and 713 mAh·g^{-1} (415 and 303 mAh·g^{-1}, calculated with the whole electrode), respectively. There is a rapid capacity decay at the initial ten cycles (0.7% per cycle). The decay rate decreases by 0.14% per cycle for the later 140 cycles, which is obviously lower than the values on other CNTs/S cathode (0.36% [35], 0.63% [19], 0.67% [23], 0.76% [34] per cycle) reported in literatures. A two-step discharging behavior was clearly observed, in which two typical plateaus at 2.44 and 1.98 V could be assigned to the two-step reaction of sulfur with lithium (Figure 4b). The positions of the plateaus were in accordance with the typical peaks of the CNT@S electrodes as shown in the CV profiles (Figure 3). The polarization behavior became more obviously with the increase of the cycle number.

Originated from the good electron pathway and effective combination of CNTs and sulfur, the CNT@S cathode afforded an excellent rate capability, as indicated in Figure 4(a). The CNT@S cathode offered a discharging capacity of 1020 mAh·g^{-1} (434 mAh·g^{-1}, calculated with the whole electrode) at a current density of 0.5 C (0.209 mA·cm^{-2}). This was larger than most discharging capacities of nanocarbon/sulfur electrodes, such as binder-free CNT-S electrode prepared by sulfur powder melting (ca. 700 mAh·g^{-1} at C/47) [37], SWCNT@S cathode (ca. 676 mAh·g^{-1} at 0.5 C in 1,3-dioxolane : 1,2-dimethoxyethane electrolyte) [35], polymer wrapped graphene-sulfur particles (ca. 580 mAh·g^{-1}) [14], and graphene enveloped sulfur (ca. 550 mAh·g^{-1} at 0.2 C) [16], and competitive to a nanocomposite with sulfur entrapped into hierarchical porous graphene (ca. 1068 mAh·g^{-1} at 0.5 C) [15], and graphene/single-walled CNTs-sulfur composite cathode (ca. 1010 mAh·g^{-1} at 0.5 C) [26]. A two-step discharging behavior was clearly observed, in which two typical plateaus at 2.44 and 2.02 V are attributed to the

two-step reaction of sulfur with lithium (Figure 5b). There were also two plateaus in the charge process at about 2.24 and 2.36 V. The capacity decreased and the over-discharged phenomenon dramatically dwindled with the increase in the charge-discharge current density (Figure 5b). The discharging capacity corresponded to the two typical plateaus decreased simultaneously. When a very high current density of 5.0 C (2.09 mA·cm^{-2}) was applied on the CNT@S electrode, a discharging capacity of 172 mAh·g^{-1} (73 mAh·g^{-1}, calculated with the whole electrode) was preserved (Figure 5a). With the increase in the discharging current, the higher order lithium polysulfide reduction rapidly decayed, and polarization phenomena became gradually significant (Figure 5b). This can be partly attributed to the slow rate of Li ion diffusion in the TEGDME based electrolyte.

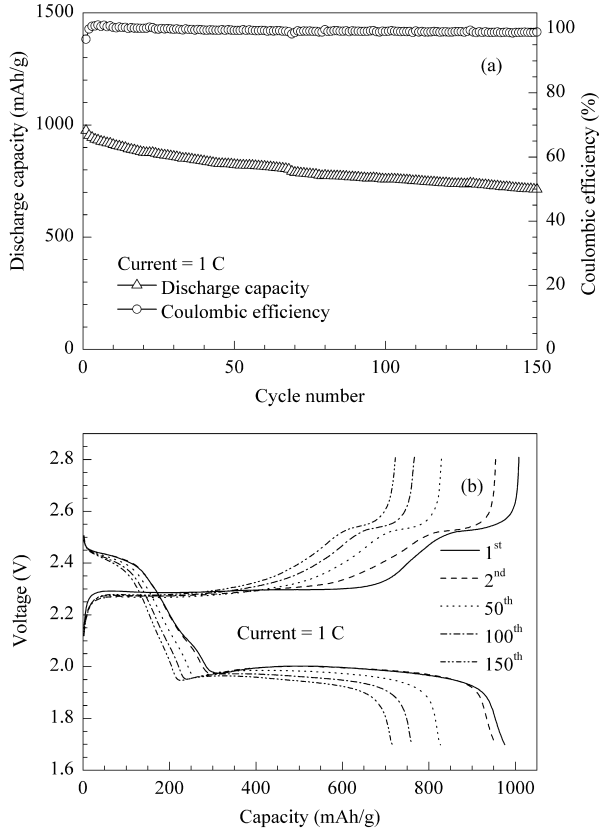

Figure 4. (a) Cycling performance and (b) galvanostatic charge-discharge curves of the reversible charge-discharge process at different cycles

With the facile co-heating of industrial produced CNTs and sulfur powder at 155 °C, the hierarchical CNT@S coaxial nanocables with three-dimensional multi-stage agglomerated nanoarchitectures were formed. In the composite, the CNTs offer conductive network for interconnected electron pathway, while the uniformly coated sulfur is active for reversible Li-ion storage. However, such a nanostructured composite cathode has not been fully optimized yet. The use of CNTs with abundant mesopores for rapid ion migration pathway is expected to present improved rate performance. Activated CNTs with a large amount of micropores that act as solvent-restricted reactors for sulfur lithiation are also promising in building electrodes with high capacity and long cycle stability. Meanwhile the graphitic walls of CNTs contribute significantly to low-resistance electron transfer [10]. The cathode nanostructure can be further improved by cathode structure modulation, architectural form-like current collector, as well as electrolyte optimization. Such hierarchical agglomerated CNT@S coaxial nanocables are of advantages in low cost, large scale production, and good electrochemical activity for Li ion storage, which are promising candidates for high performance Li-S battery.

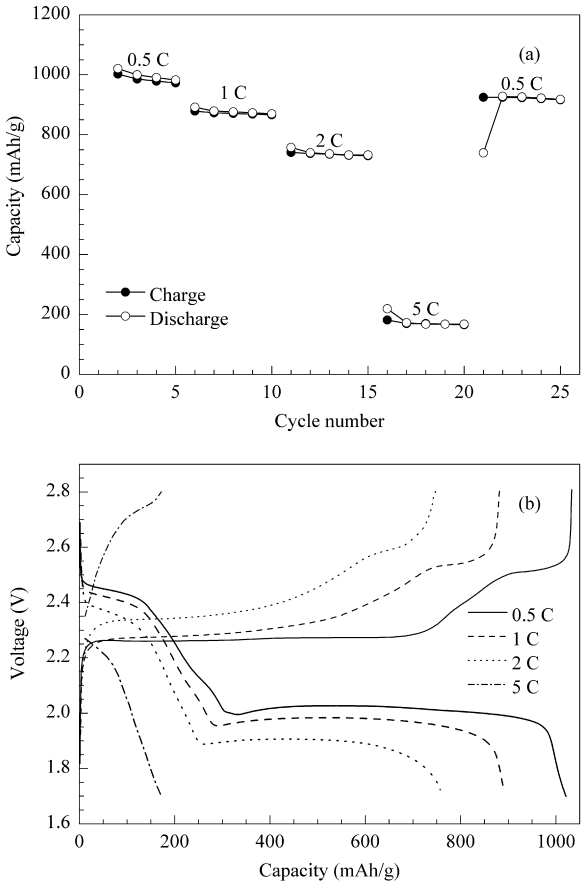

Figure 5. Rate performance (a) and galvanostatic charge-discharge curves (b) of the reversible charge-discharge process

4. Conclusions

A nanocomposite cathode containing CNT@S coaxial nanocables with a 1st discharging capacity of 1020 mAh·g^{-1} at 0.5 C, a 150th discharging capacity of 713 mAh·g^{-1} at 1.0 C, and a discharging capacity of 740 mAh·g^{-1} at 2.0 C was fabricated by a facile one-step melt-diffusion strategy based on industrial produced CNTs. Such a hierarchical CNT@S cathode is of advantages in facile fabrication, environmentally benign, low cost, excellent scalability, and good Li ion storage performance, which is a promising market ready cathode for Li-S battery. Furthermore, the CNTs-based

coaxial nanocables can be an important structural platform for nanocomposites with robust electron and ion pathway for heterogeneous catalysts, electrochemical energy storage, and other related applications.

Acknowledgements

This work was supported by the National Basic Research Program of China (973 Program, 2011CB932602), Research Fund for the Doctoral Program of Higher Education of China (20120002120047), and China Postdoctoral Science Foundation (2012M520293).

References

[1] Su D S, Schloegl R. *ChemSusChem*, 2010, 3(2): 136
[2] Bruce P G, Freunberger S A, Hardwick L J, Tarascon J M. *Nat Mater*, 2012, 11(1): 19
[3] Evers S, Nazar L F. *Accounts Chem Res*, 2013, doi: 10.1021/ar3001348
[4] Manthiram A, Fu Y Z, Su Y S. *Accounts Chem Res*, 2013, doi: 10.1021/ar300179v
[5] Yao Z D, Wei W, Wang J L, Yang J, Nuli Y N. *Acta Phys Chim Sin*, 2011, 27(5): 1005
[6] He X M, Ren J G, Wang L, Pu W H, Jiang C Y, Wan C R. *J Power Sources*, 2009, 190(1): 154
[7] Zhao M Q, Zhang Q, Huang J Q, Wei F. *Adv Funct Mater*, 2012, 22(4): 675
[8] Ji X L, Lee K T, Nazar L F. *Nat Mater*, 2009, 8(6): 500
[9] Wang J L, Liu L, Ling Z J, Yang J, Wan C R, Jiang C Y. *Electrochim Acta*, 2003, 48(13): 1861
[10] Wang D W, Zhou G M, Li F, Wu K H, Lu G Q, Cheng H M, Gentle I R. *Phys Chem Chem Phys*, 2012, 14(24): 8703
[11] Barchasz C, Mesguich F, Dijon J, Lepretre J C, Patoux S, Alloin F. *J Power Sources*, 2012, 211: 19
[12] Liang X, Wen Z Y, Liu Y, Wu M F, Jin J, Zhang H, Wu X W. *J Power Sources*, 2011, 196(22): 9839
[13] Zhang B, Qin X, Li G R, Gao X P. *Energy Environ Sci*, 2010, 3(10): 1531
[14] Wang H L, Yang Y, Liang Y Y, Robinson J T, Li Y G, Jackson A, Cui Y, Dai H J. *Nano Lett*, 2011, 11(7): 2644
[15] Huang J Q, Zhang Q, Liu X F, Chen C M, Zhao M Q, Zhang S M, Zhu W C, Qian W Z, Wei F. *Nano Energy*, 2013, 2(2): 314
[16] Evers S, Nazar L F. *Chem Commun*, 2012, 48(9): 1233
[17] Wu F, Wu S X, Chen R J, Chen S, Wang G Q. *New Carbon Mater*, 2010, 25(6): 421
[18] Ahn W, Kim K B, Jung K N, Shin K H, Jin C S. *J Power Sources*, 2012, 202: 394
[19] Yuan L X, Yuan H P, Qiu X P, Chen L Q, Zhu W T. *J Power Sources*, 2009, 189(2): 1141
[20] Chen J J, Zhang Q, Shi Y N, Qin L L, Cao Y, Zheng M S, Dong Q F. *Phys Chem Chem Phys*, 2012, 14(16): 5376
[21] Dorfler S, Hagen M, Althues H, Tubke J, Kaskel S, Hoffmann M J. *Chem Commun*, 2012, 48(34): 4097
[22] Wei W, Wang J L, Zhou L J, Yang J, Schumann B, NuLi Y N. *Electrochem Commun*, 2011, 13(5): 399
[23] Guo J C, Xu Y H, Wang C S. *Nano Lett*, 2011, 11(10): 4288
[24] Kim H, Lee J T, Yushin G. *J Power Sources*, 2013, 226: 256
[25] Zheng G Y, Yang Y, Cha J J, Hong S S, Cui Y. *Nano Lett*, 2011, 11(10): 4462
[26] Zhao M Q, Liu X F, Zhang Q, Tian G L, Huang J Q, Zhu W C, Wei F. *ACS Nano*, 2012, 6(12): 10759
[27] Yin L C, Wang J L, Yang J, Nuli Y N. *J Mater Chem*, 2011, 21(19): 6807
[28] Wu F, Chen J Z, Li L, Zhao T, Chen R J. *J Phys Chem C*, 2011, 115(49): 24411
[29] Zhang Q, Huang J Q, Zhao M Q, Qian W Z, Wei F. *ChemSusChem*, 2011, 4(7): 864
[30] Huang J Q, Zhang Q, Zhao M Q, Wei F. *Chin Sci Bull*, 2012, 57(2-3): 157
[31] Wang X Y, Zhang J C, Zhu H. *Chin J Catal (Cuihua Xuebao)*, 2011, 32(1): 74
[32] Yin S B, Zhu Q Q, Qiang Y H, Luo L. *Chin J Catal (Cuihua Xuebao)*, 2012, 33(2): 290
[33] Zheng C, Qian W Z, Cui C J, Xu G H, Zhao M Q, Tian G L, Wei F. *J Nat Gas Chem*, 2012, 21(3): 233
[34] Han S C, Song M S, Lee H, Kim H S, Ahn H J, Lee J Y. *J Electrochem Soc*, 2003, 150(7): A889
[35] Zhang S M, Zhang Q, Huang J Q, Liu X F, Zhu W C, Zhao M Q, Qian W Z, Wei F. *Part Part Syst Char*, 2013, 30(2): 158
[36] Zhou G M, Wang D W, Li F, Hou P X, Yin L C, Liu C, Lu G Q, Gentle I, Cheng H M. *Energy Environ Sci*, 2012, 5(10): 8901
[37] Hagen M, Dorfler S, Althues H, Tubke J, Hoffmann M J, Kaskel S, Pinkwart K. *J Power Sources*, 2012, 213: 239
[38] Hagen M, Dorfler S, Fanz P, Berger T, Speck R, Tubke J, Althues H, Hoffmann M J, Scherr C, Kaskel S. *J Power Sources*, 2013, 224: 260
[39] Wei F, Zhang Q, Qian W Z, Yu H, Wang Y, Luo G H, Xu G H, Wang D Z. *Powder Technol*, 2008, 183(1): 10
[40] Aurbach D, Pollak E, Elazari R, Salitra G, Kelley C S, Affinito J. *J Electrochem Soc*, 2009, 156(8): A694
[41] Xiong S Z, Xie K, Diao Y, Hong X B. *Electrochim Acta*, 2012, 83: 78
[42] Zhang S S. *J Electrochem Soc*, 2012, 159(7): A920